On-line tool condition monitoring in face milling using current and power signals

P. BHATTACHARYYA*†, D. SENGUPTA†, S. MUKHOPADHYAY‡
and A. B. CHATTOPADHYAY§

†Applied Statistics Unit, Indian Statistical Institute, 203, B.T. Road,
Kolkata, India 700108
‡Department of Electrical Engineering, I.I.T., Kharagpur, India 721302
§Department of Mechanical Engineering, I.I.T., Kharagpur, India 721302

The vast majority of tool condition monitoring systems use the cutting force as the predictor signal. However, due to prohibitive cost to performance ratios and maintenance and operational problems, such methods are not favoured by industries. In this paper, a method for continuous on-line estimation of tool wear, based on the inexpensive spindle motor current and voltage measurements, is proposed for the complex and intermittent cutting face milling operation. Sensors for these signals are free from problems associated with the cutting forces and the vibration signals. Novel signal processing strategies have been proposed for on-line computation of useful features from the measured signals. Feature space filtering is introduced to obtain robust and improved predictors from the extracted features. A multiple linear regression model, built on the filtered features, is then used to estimate tool wear in real-time. Very accurate predictions are achieved for both laboratory and industrial experiments, surpassing earlier results using cutting forces and estimation methods based on complex methodologies such as artificial neural networks.

Keywords: Tool wear; Real-time tool condition monitoring; Signal processing; Multiple linear regression

1. Introduction

Ensuring product quality and reducing machine downtime is paramount for survival of any manufacturing industry. Moreover, the state-of-the-art machine tools are very expensive and so, the manufacturers try to reduce unplanned breakages of the production process to obtain faster return on investment. Tool wear, especially flank wear, adversely impacts accuracy and surface finish of the machined products (Ulsoy and Koren 1993). Also, time required for changing and resetting of the worn tools constitutes nearly 20% of a machine's downtime (Karuda and Bradley 1997). Additionally, tool life is short and has considerable variations (Bukkapatnam *et al.* 2000). For these reasons, quality and productivity of a machining process is enhanced effectively by optimising the tool changing schedule. This requires accurate

on-line estimation of tool wear based on measurement of process signals such as, cutting forces, vibrations, spindle motor current and voltage, acoustic emission (AE) etc. Industrial acceptability of a method of on-line tool condition monitoring (OLTCM) crucially depends on the cost and the maintainability of the sensors as with the associated operational issues, such as mounting, environmental protection, noise immunity, etc.

Dimla 2000 reviewed the effects of different process signals on tool wear. Balazinski *et al.* (2002) showed the cutting forces to be more effective indicator of tool condition than acoustic emission and vibration signals for the turning process. Szecsi (1998) estimated flank wear using offline measurement of the axial cutting force and a linear regression model. Dutta *et al.* (2000a, b) proposed a TCM scheme for face milling operation based on cutting forces, speed, feed and depth of cut, using artificial neural network (ANN). Saglam and Unuvar (2003) proposed an ANN-based TCM in face milling using the cutting forces. However, Bukkapatnam *et al.* (2000) reported that the existing architectures of neural networks are extremely complicated, entail significant computational overheads and are not guaranteed to converge. Inasaki and Fuduoka (1987) developed a method for the detection of tool chipping using the power spectrum of the AE signals. Sun *et al.* (2004) identified effective feature set from the AE signal using Bayesian framework and support vector machine. Prickett and Johns (1999) suggested use of the classical multi-sensor fusion and integration of control signals by the machine numerical controller. Chen and Jen (2000) developed TCM for CNC milling using the forces and the vibration signals. Dimla and Lister (2000a, b) also considered the cutting forces and the vibration signals in both time and frequency domains. Recently, the wavelet transform (WT) and the fuzzy decision paradigms were used for TCM, especially for tool breakage detection and wear estimation. Pittner *et al.* (1998) investigated assessment of wear in turning through force and vibration signals using a wavelet network. Kamarthi *et al.* (2000) used wavelet representation of the AE signals for estimation of wear in turning using recurrent neural networks. Li *et al.* (2000) attempted distinction of sharp tools from the worn ones using wavelet transform of the vibration signals and a hidden Markov model (HMM). Wang *et al.* (2002) also used HMMs for tool state classification using the vector quantisation of the features from vibration signals. In Bukkapatnam (2000), tri-axes cutting forces, vibration and AE signals were used for estimation of tool wear using wavelet based signal separation and fractal properties of the machine dynamics.

Recent reviews (Scheffer and Heyns 2001, Sick 2002) indicate that most of the TCM systems employed force, AE and vibration or a combination of these signals. However, the sensors for the force signals, i.e. the dynamometers, are expensive and have to be placed either on the workpiece holder or the tool holder. As a result, these sensors pose mounting and operational problems and may severely restrict the maximum size of the job that can be handled by the machine. Consequently, the cutting force based estimation methods are not favoured by the industry. On the other hand, sensors for vibration and AE signals have to be placed close to the machining area for effective signal pick up and are prone to accidental damage. Also, these sensors are sensitive to environmental noise. Current and power signals from the spindle motor are free from such limitations and hence could be effective alternatives for OLTCM. The literature using the electrical signals for TCM are

sparse and mostly attempted either tool breakage detection or tool state classification, which are inherently simpler.

Tool breakage detection was attempted in Altintas (1992) and Lee *et al.* (1995). Ertunc *et al.* (2001) and Jeong and Cho (2002) proposed on-line classification of tool states based on the cutting force using HMMs. In Jeong and Cho (2002), predicting condition of the cutting tools using the feed motor current alone proved unsuccessful. Romerio-Troncoso *et al.* (2003) proposed a method for detection of broken or worn tools using the feed motor current. The related analysis was relatively simple as the drive was a DC one and the assumed signal model was additive. Further it did not attempt continuous wear estimation. In another recent work also, Ghosh *et al.* (in press) developed a TCM for face milling using the cutting forces and failed to extract useful information from the current signal. The reported correlation of the force and the current was 0.08 and 0.076 in that work, which is useless for the purpose of building tool wear model.

The present work stemmed from these considerations. It aims at

- replacing the cutting force signal as predictor of tool wear by the non-invasive and inexpensive spindle motor current and voltage measurements for the complex and intermittent face milling operation;
- development of an accurate and reliable estimator for continuous assessment of tool wear based on these alternate measurements;
- use of novel signal processing methods such as estimation of line frequency, demodulation and segmentation for extraction of useful information from the acquired electrical signals;
- use of time domain features for efficient real time computation;
- use of a new feature space filtering technique to enhance robustness and accuracy of the predictors;
- use of linear prediction through multiple linear regression (MLR) modelling;
- providing probabilistic upper bounds (prediction limits) for the estimates, thereby indicating the worst case predictions of tool wear;
- using data from industrial setups to show applicability of the method for real working environment.

It is found from the results that the proposed method compares favourably with those reported in the literature and those utilising force measurements.

Organisation of the paper is as follows. Section 2 of the paper presents the experimental setup. Section 3 details the signal processing steps for the electrical signals. Section 4 deals with extraction and filtering of features and prediction model. Results and prediction limits are detailed in section 5. Finally, some concluding remarks are made in section 6.

2. Experimental setup

Two datasets, from tool life experiments conducted on a conventional face-milling machine in the laboratory of the Indian Institute of Technology, Kharagpur, and an industrial CNC Plano-miller at the Flenders Limited, Kharagpur, are used in this work. These are called datasets I and II respectively in the paper. The details of machining parameters are given in table 1.

Table 1. Machining parameters.

	Dataset I	Dataset II
Cutting speed (m/min)	140	212
Feed (mm/rev)	0.22	0.16
Depth of cut (mm)	1.5	2.4
Max wear value (micron)	631	370
Workpiece material	C-60 mild steel	
Cutter diameter (mm)	125	
Cutting condition	Dry	
Number of inserts	One	

Machining operations were stopped at intervals and wear values were measured with an optical microscope with a least count of 1 micron. Forces were sensed using a Kistler 3-axes dynamometer. Current and voltage were measured using Kistler Hall effect current and voltage sensors. A sampling frequency of 35 kHz was used for both the experiments. In a dataframe, i.e. the measurements for a single observed wear value, there are 32 768 data points corresponding to a time span of 0.94 seconds. The wear limit for finish machining is taken as 300–400 microns, while the same for rough machining is 600–800 microns (Elbestawi *et al.* 1998). For this reason, 98 and 18 observations of wear values were recorded in the ranges of 0–631 and 0–370 microns for the two datasets respectively, so that the developed model need not be used beyond the observed range of wears during actual operation.

3. Signal processing

3.1 *Process signals*

3.1.1 Cutting forces in feed and transverse directions. The cutting forces in the direction of feed (F_x, figure 1a) and in the transverse direction (F_y, figure 1b) in the cutting plane are periodic with a fundamental frequency corresponding to the spindle rotational speed. Due to intermittent cutting operation, the measurements have distinct cutting durations, called lobes, in every cycle. Noise is introduced in the signal due to factors such as vibration, non-uniformity of the workpiece and the tool materials, sensor noise, etc. The force signals yield accurate estimates of tool wear due to their high signal-to-noise ratios (SNR). Though the cutting durations of the signal are mainly relevant for estimation, signals are considered beyond the cutting durations to include transients during tool disengagement time also (Altinas *et al.* 1988). The force signals are segmented in the same way as in Ghosh *et al.* (in press). Then the extracted features are filtered by exponential smoothing (section 4) to improve performance and fed to multiple linear regression models for estimation. These models are used to compare performance of the models developed based on the electrical signals.

3.1.2 Spindle motor line current and input power. The instantaneous current signal (figure 2a) appears to consist mainly of the ac line frequency component.
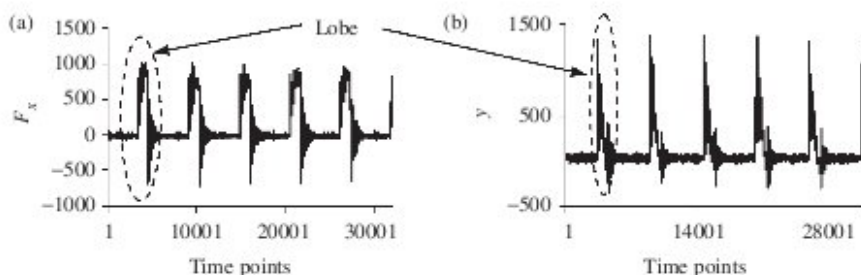
Figure 1. (a) F_x and (b) F_y vs. time points for a typical dataframe.
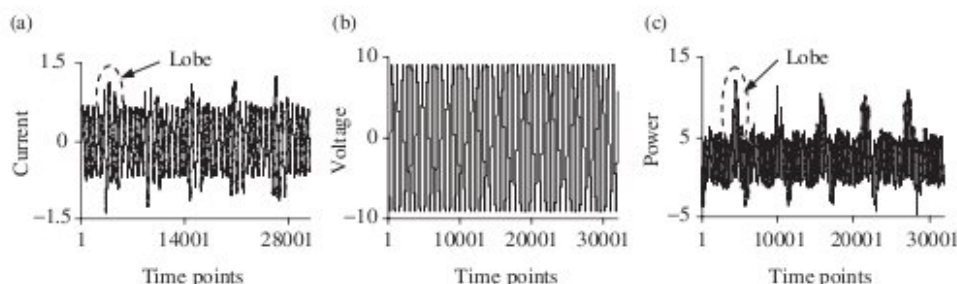

Figure 2. Time plots of (a) the current, (b) the voltage and (c) the power respectively vs. time points for a typical dataframe.

It is amplitude modulated by the periodic rise in torque demand during the cutting periods, which occurs at a frequency of 2–10 Hz depending on the rotational speed of the cutter. There are non-cutting durations in between the consecutive cutting durations due to intermittent cutting.

The current is therefore modelled as

$$I_i = A(1 + m(t_i))\cos(2\pi f t_i + \theta_1), \quad i = 1, \ldots, N \tag{1}$$

where, the constant A represents the no-load current, $m(t_i)$ represents the time-varying modulation index, f, the line frequency and θ_1, the phase.

The instantaneous power is defined as the product of instantaneous current and voltage signals. The latter appears as a line frequency sinusoid given by

$$V_i = B\cos(2\pi f t_i + \theta_2), \quad i = 1, \ldots, N \tag{2}$$

relatively unaffected by the cutting process as in figure 2(b). The instantaneous power shown in figure 2(c) is, therefore, modelled as a product of (1) and (2) as

$$P_i = C(1 + m(t_i)) + D(1 + m(t_i))\cos(4\pi f t_i + \phi), \quad i = 1, \ldots, N \tag{3}$$

C, D, f and ϕ being constants. It contains components corresponding to the low frequency of the cutting force given by the first term of (3) and components centred on twice the line frequency given by the other term.
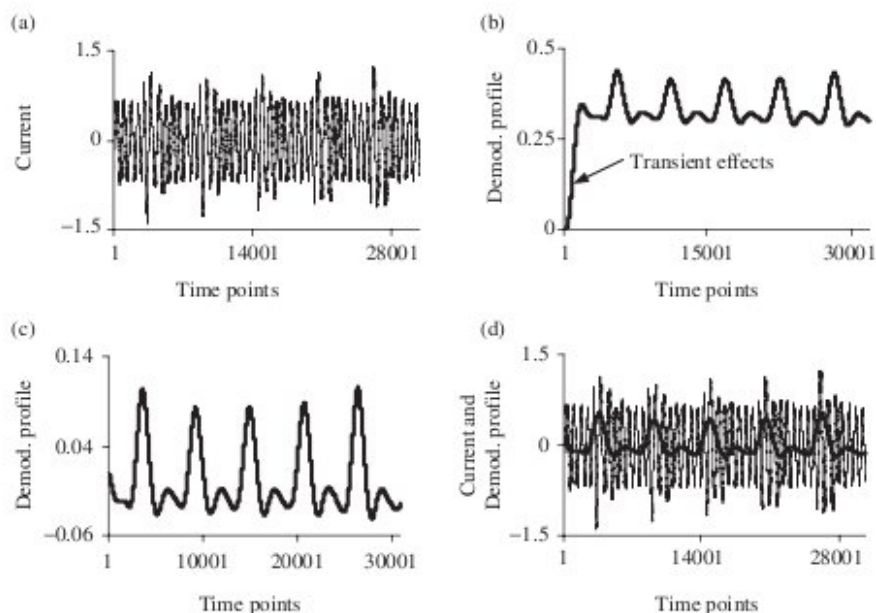
P. *Bhattacharyya* et al.

Figure 3. Time plots of (a) the original current signal, (b) the demodulated profile, (c) the demodulated profile after removal of transient effects and drift and (d) the original current signal (thinner line) superimposed with preprocessed demodulated profile for a typical dataframe.

3.2 *Pre-processing of signals*

Tool wear takes place during the cutting operation only. So, the non-cutting portions of the electrical signals are noise from the point of estimation of tool wear. It is, thus, necessary to segment the measured signals to retain only cutting lobes. The line frequency component of the current makes it difficult to identify the start or the end of the cutting lobes. Thus, it is necessary to extract the modulating profile $m(t_i)$ by demodulating the acquired current and the power measurements.

3.2.1 Demodulation of the current signal. De-modulation of the current involves (i) point to point multiplication of the measured signal by the estimated 'carrier' as the first step and (ii) linear filtering in the second step (Lathi 1968). As the dominant component of this signal is a sinusoid at the line frequency, frequency and phase of the carrier are estimated by minimising the error sum of squares, given by

$$e^2 = \sum_i (y_i - a_1\sin(2\pi f t_i) - a_2\cos(2\pi f t_i))^2 \qquad (4)$$

over f, a_1 and a_2. For given f, values of a_1 and a_2 can be optimised by linear least squares estimation (LSE). The value of f can then be optimised by minimising this partially optimised sum of squares within a frequency range of 48 to 52 Hz, first over a coarse grid over the whole range and then, over successively finer grids. The use of

LSE reduces the three-dimensional optimisation (over a_1, a_2 and f) to a one-dimensional search over f only. The phase is then calculated as $\theta_1 = \tan^{-1}(-a_2/a_1)$.

For the industrial dataset, a lot of high frequency noise is introduced in the current measurement due to the power electronic switching. The original measurement is therefore filtered with a 4th order low-pass Butterworth filter with a cut off frequency of 61.25 Hz, prior to estimation of the line frequency.

After estimation of the frequency and the phase of the carrier sinusoid, demodulation of the current is achieved by multiplication of the instantaneous measured signal with the instantaneous carrier sinusoid of the estimated frequency and phase and then, by low-pass filtering the resultant product signal. In this work, a 4th order Butterworth filter of cut off frequency 17.5 Hz is used for low pass filtering, as the highest cutting frequency in the current is limited to 10 Hz. Transient effects (figure 3b), introduced due to the filtering, are removed by dropping a few initial sample points from the demodulated profile. Drift, present in the demodulated signal, is eliminated by subtracting a least squares fitted line from it (figure 3c). Similarity between the resultant demodulated signal and the amplitude envelope of the measured signal is shown in figure 3(d). As the calculated frequency is a single value for the entire dataframe and it varies from the true frequency in different parts in the frame, the demodulated profile suffers from distortion wherever there is either frequency or phase mismatch. For this reason, the demodulated profile has been used only to segment the original current signal.

3.2.2 Filtering of the power signal. Instantaneous power signal, being product of the instantaneous current signal given by (1) and the instantaneous voltage signal given by (2), is 'demodulated' simply by low-pass filtering with a 4th order low-pass Butterworth filter of cut off frequency of 17.5 Hz. The filtered power signal in figure 4 is seen to be very similar to the profiles of cutting forces in figures 1(a) and (b).

3.3 *Segmentation*

Segmentation involves (i) elimination of the incomplete lobes from the demodulated profile of each measured dataframe, (ii) identifying time points that indicate the beginning and the end of each complete lobe in it and (iii) temporal registration of the complete lobes of the measured dataframes with those of the corresponding demodulated profile. In face milling, the electrical signals achieve peak values near the middle of a complete lobe. Accordingly, in the demodulated profile (figure 5), a complete lobe is taken to be the signal segment between two successive minima (points 'b_1' and 'b_2' respectively) on the two sides of a maximum (points marked 'a'), above a chosen threshold. The threshold is dynamically calculated for each dataframe as 0.7 times (i.e. nearly 3dB below) the maximum signal value in the signal span corresponding to one revolution of the cutter, from the beginning of the dataframe. If either of the two minima is missing, that cutting lobe is rejected as an incomplete one. The process is depicted in figure 5. Finally, we pick up the lobes in the measured signal by temporal registration with the segmented demodulated profile, as the latter has a fixed offset with respect to the former in all the dataframes (see figure 3d).
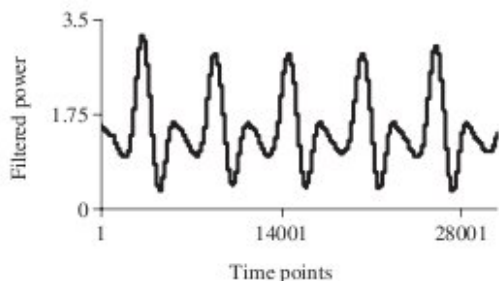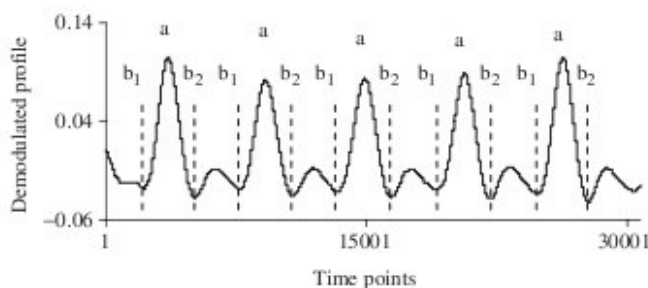
P. Bhattacharyya et al.

Figure 4.   Filtered power signal.

Figure 5.   Segmentation process—points 'b₁' and 'b₂' indicate the start and the end of a complete cutting lobe and points 'a' mark the middle of cutting lobes.

4. Filtered features and prediction model

A worn tool requires more energy for cutting compared to a fresh one. Accordingly, features representative of the cutting energy, e.g. the average signal energy over the complete lobes in a dataframe, are considered as the candidate features. Several features, such as, average mean squared value (s_{amj}) and average variance (s_{avj}) for current and force signals and the average root mean squared value (t_{amj}) and the mean standard deviation (t_{avj}) for power signal, have been considered. The mathematical representations of the features are given below.

Let a_{ijk} be the signal value at the kth sample point and n_{ij} be the number of data points in the i-th cutting lobe of the jth dataframe, where $i = 1, \ldots, N_j$, N_j being the number of complete lobes in the frame. Then, for the current signal,

$$f_{ij} = \frac{\sum_{k=1}^{n_{ij}} a_{ijk}^2}{n_{ij}} \quad s_{amj} = \frac{\sum_{i=1}^{N_j} f_{ij}}{N_j}$$

$$a_{mi} = \frac{\sum_{k=1}^{n_{ij}} a_{ijk}}{n_{ij}} \quad b_{ij} = \sqrt{\frac{\sum_{k=1}^{n_{ij}} (a_{ijk} - a_{mi})^2}{(n_{ij} - 1)}} \quad s_{avj} = \frac{\sum_{i=1}^{N_j} b_{ij}^2}{N_j}$$

Similarly for the power signal,

$$g_{ij} = \sqrt{\frac{\sum_{k=1}^{n_{ij}} a_{ijk}^2}{n_{ij}}} \quad t_{anj} = \frac{\sum_{i=1}^{N_j} g_{ij}}{N_j}$$

$$a_{mi} = \frac{\sum_{k=1}^{n_{ij}} a_{ijk}}{n_{ij}} \quad b_{ij} = \sqrt{\frac{\sum_{k=1}^{n_{ij}} (a_{ijk} - a_{mi})^2}{(n_{ij} - 1)}} \quad t_{avj} = \frac{\sum_{i=1}^{N_j} b_{ij}}{N_j}$$

These features are chosen on the basis of their correlation with the observed wear values. For the sake of brevity, the results corresponding to the feature s_{amj} are given in (a) above, for the current and the force and the feature t_{amj} for the power, are presented here. The trend of the extracted or 'raw' features against the observation points for dataset I is depicted in figure 6(a). The drop from observation point 44 to 57 is due to power fluctuation that took place during the data acquisition phase (Ghosh *et al.* in press).

Tool wear is essentially a continuous and monotonic phenomenon. The high frequency variations in the raw features (see figure 6a) are therefore smoothed to obtain a better predictor. The smoothed feature is computed as

$$y_i = \frac{\sum_{j=0}^{i} w^j x_{i-j}}{\sum_{j=0}^{i} w^j} \tag{5}$$

where, w ($0 < w < 1$) is a predefined weighting factor (0.99 in the present case) and x_i is the raw feature value corresponding to i-th observation of wear. The final features are obtained from the smoothed features by normalisation with respect to the largest value for the dataset. The trends of raw and final features from the current for dataset I are presented in figures 6(a) and (b) to bring out the improvement due to smoothing. The improvement in correlation coefficients of the final features based on the current and the power are 22% and 23% for dataset I respectively and 17.5% and 16% for dataset II respectively.

For initial observations, filtering is inadequate due to lack of past data. But this does not affect performance of the estimator as the tool is fresh in this area of operation and estimated wear values need not be accurate. For dataset I, there was a sudden voltage drop in the middle part of data acquisition (Ghosh *et al.* in press) that affected all features based on the electrical signals. Such supply variations, being realistic, have not been omitted from the estimation. Force signals, however, are unaffected by such disturbances.

The filtered features are used as explanatory variables in a multiple linear regression model (Sengupta and Jammalamadaka 2003, Montgomery *et al.* 2003) of the form

$$y_i = \hat{\beta}_0 + (\hat{\beta}_1 \times x_{i1} + \cdots + \hat{\beta}_p \times x_{ip}) + e_i \tag{6}$$

where y_i is the i-th observed wear value, x_{ij} is the j-th smoothed and normalised feature value for the same i-th observation, $\hat{\beta}_0$, $\hat{\beta}_1$ are the unspecified model parameters, and $e_1, \ldots, e_n$ are model errors representing measurement error, effects of omitted variables, etc. The methodology for analysis under this simple prediction model using the least squares technique is well developed. Assuming that the
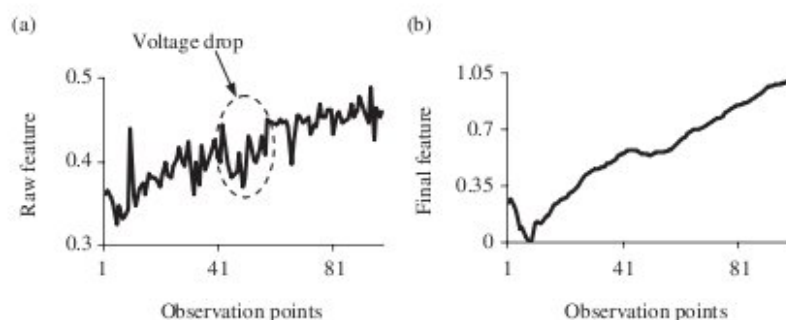
Figure 6.　Trends of (a) the raw and (b) the final features from the current signal for dataset I.

residuals follow a given probability distribution, probabilistic bounds of wear values for a given feature profile can also be provided on the basis of this model.

5. Results and prediction limits

5.1 *Line plots of the estimated and observed wears*

The estimation is quite accurate as is seen from the line plots of the estimated and the observed wears shown in figure 7(a) to (d) for dataset I and in figure 8(a) to (d) for the dataset II. In spite of power supply fluctuations during middle part of dataset I, the errors are small over the entire range of application. Large errors are few in number and are largely limited to initial values of wear. As the tool is fresh in this part of machining, it is not important and also impact of these errors on subsequent prediction is seen to be negligible. The performance of the models using the electrical signals is comparable, in terms of magnitude of errors and their distribution across the range of observed wears, to that based on the force signal. Since fewer sample points were available for dataset II (due to constraint of allowed time for the experiment), deviations from the observed values are larger compared to dataset I. However, even for this small number of sample points, which are adequate for the regression analysis, the performance of the method is reasonably good.

5.2 *Regression results*

The results of regression analysis are given in table 2 in the form of multiple correlation (R) and the factor of determination, i.e. R^2. The multiple correlation designates the degree of linear dependence between the response variable i.e. observed wear values and the explanatory variables i.e. extracted feature values. The R^2 values indicate the fractions of the total variances that are explained by the models. From the results, it is seen that all the predictors perform very well. The R^2 values for the features extracted from the electrical signals are comparable to that from the force signal. Combination of features from current and power signals provides improvement over models from any of the individual signals.
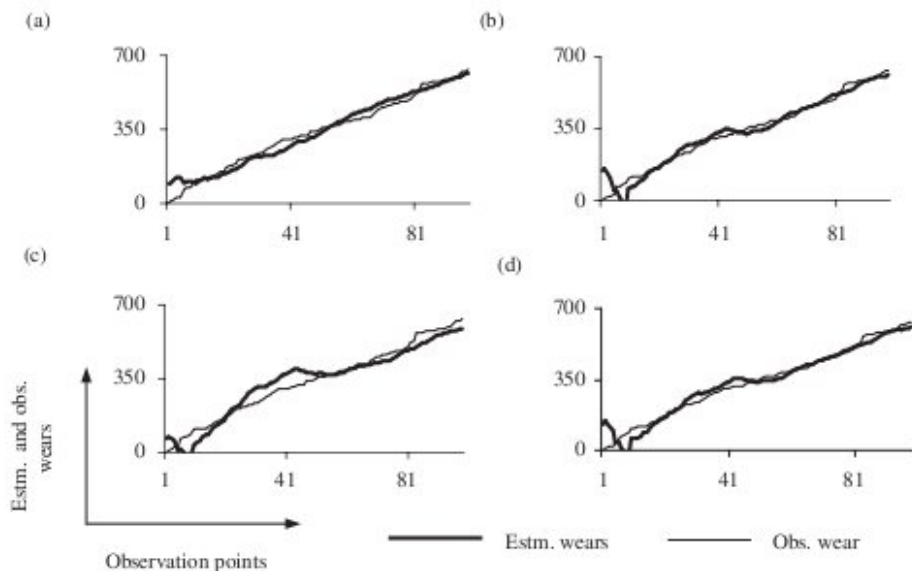
Figure 7. (a)–(d). The observed and the estimated wear values in microns vs. observation points for (a) force, (b) current, (c) power and (d) combination of current and power signals respectively, for dataset I.
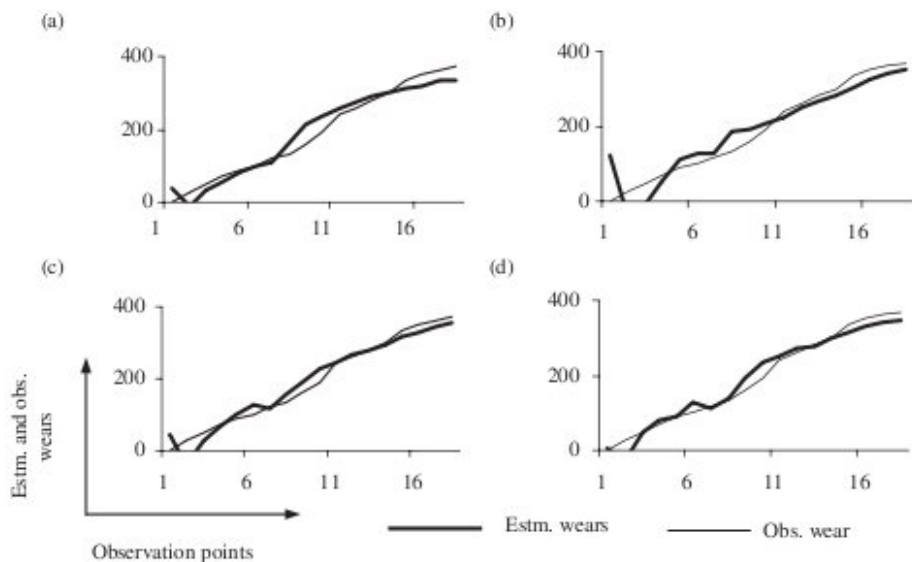

Figure 8. The observed and the estimated wear values in microns vs. observation points for (a) force, (b) current, (c) power and (d) combination of current and power signals respectively, for dataset II.

Table 2.   Regression results (figures rounded up to two decimal places).

	Laboratory dataset				Industry dataset			
	A	B	C	D	A	B	C	D
Multiple correlation (R)	0.98	0.98	0.97	0.98	0.98	0.94	0.98	0.98
R^2	0.96	0.96	0.93	0.96	0.94	0.88	0.96	0.97

A, Force (F_x); B, Current; C, Power; D, Combination of current and power.

Table 3.   Error statistics (in microns).

	Laboratory dataset				Industrial dataset			
	A	B	C	D	A	B	C	D
LAE	104	153	108	136	52	124	63	54
AAE	26	23	36	24	23	32	19	16
AAE1	22	16	33	18	22	22	15	15
SE	32	36	44	35	29	44	27	24

A, Force (F_x); B, Current; C, Power; D, Combination of current and power.

5.3 Error statistics

In table 3, the largest absolute errors (LAE), the average absolute errors (AAE) and the standard errors (SE) are presented. The average absolute errors are indicative of the average degree of deviation of the predicted values from the observed wears, while the standard errors are representative of the root mean squared prediction error. These values are significant improvements over those reported in the literature (Ghosh *et al.* in press). The average absolute errors improve further if some initial observations (10 for dataset I and 3 for dataset II), pertaining to a fresh tool, are ignored. This is reported as AAE1 in Table 3.

5.4 Prediction limits

Using the available features, the linear regression model and assuming that the residuals are independent and identically distributed from the normal distribution ($N(0, \sigma^2)$), one can provide a probabilistic upper bound (prediction limit) for the amount of actual wear. The upper prediction limit is useful in this case as it stands for a typical 'lower the better' degradation situation. The prediction limits and the observed wear values for the current and the power signals for the laboratory and the industrial datasets are presented in figures 9(a) to (d). The upper prediction limit with coverage probability $(1-\alpha)$ and corresponding to feature value $z=(z_1,\ldots,z_p)^T$ is given by:

$$\hat{\beta}_0 + (\hat{\beta}_1 \times z_1 + \cdots + \hat{\beta}_p \times z_p) + \sigma \times \sqrt{1+h} \times t_{\alpha,p-2} \tag{7}$$
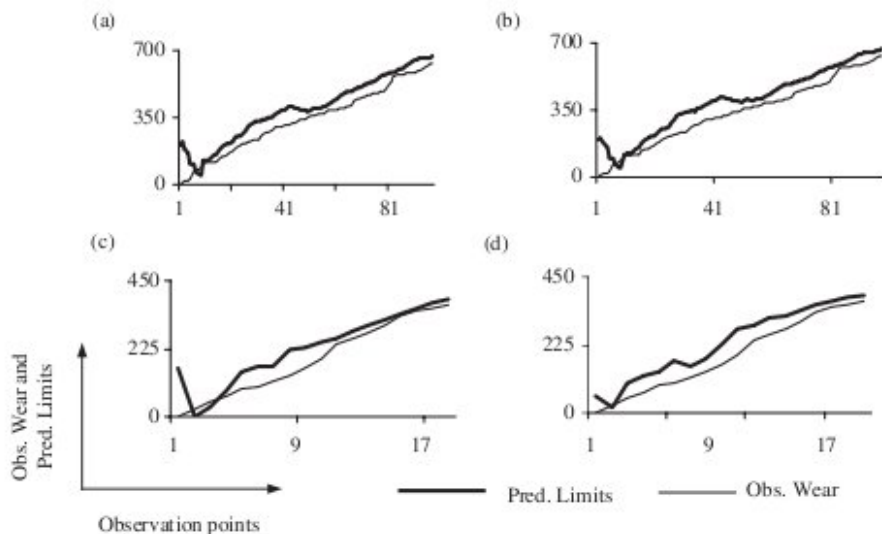
Figure 9. The observed wear values and the prediction limits in microns vs. observation points for (a) the current and (b) the combination of current and power for dataset I; (c)–(d) depict the observed wear values and the prediction limits for the same signals for dataset II.

where

$$h = (1 : z^T)(\mathbf{Z}^T\mathbf{Z})^{-1}\begin{pmatrix}1\\z\end{pmatrix}, \ X = \begin{pmatrix}1 : z_1^T\\ \vdots \\ 1 : z_n^T\end{pmatrix} \quad (8)$$

and $z_1, \ldots, z_p$ are the feature values. The results in figure 9(a) to (d) pertain to value of α equal to 0.05 and values of z corresponding to the extracted feature values only. This implies that the probability that the observed wear values would lie below the limit given by (7) is $(1 - \alpha)$, i.e. 0.95 in the present case. It is seen from the figures that the loci of the prediction limits lie generally above the actual wear values, but stay close enough to be practically useful.

6. Conclusion

In this work, an attempt is made to replace TCM methods based on cutting forces for the face milling by a new method using the inexpensive and non-invasive current and power measurements. It is seen from case studies that estimations based on current and/or power can accurately and reliably estimate tool wear for face milling operation. It is also seen that, by choice of suitable signal processing techniques, linear regression based methods using the electrical measurements are capable of providing accuracies favourable to earlier methods based on the cutting forces and ANNs. The average absolute errors for the model are significant improvements over those reported in the literature (Saglam and Unuvar 2003, Ghosh *et al*. in press).

The fit based on the electrical signals may be improved by using weighted least squares technique with weights decreasing monotonically with local variance of the estimates. However, this modification was not attempted as the ordinary least squares produced satisfactory results.

The results show that it is possible to replace the cutting force signals altogether, as indicators of tool wear, by the current and the power signals. The cutting force based models are not favoured by the industry. The proposed model, based on non-invasive and inexpensive electrical measurements and having accuracies to the tune of 95%, has potential for industrial acceptance. In this work, the same model is assumed to hold for a new tool/workpiece combination under similar cutting conditions. However, new training may be necessary for a new installation and also for significantly different cutting conditions. It may be noted that such new training is a standard feature for machining experiments.

A single cutting tool insert is used in these experiments. However, the case of multiple cutting tool inserts is a simplification over the proposed method as, in that case, the cutting lobes corresponding to the different inserts would overlap. So the segmentation step may not be needed and features could be extracted from the entire dataframe. Also two combinations of speed, feed and depth-of-cut, have been used in the work. Development of OLTCM using cutters with multiple cutting tool inserts and a range of cutting parameters would be a future extension of the work.

Acknowledgements

References

Altitas, Y., Yellowley, I. and Tlusty, J., The detection of tool breakage in milling operations. *J. Eng. Indust.*, 1988, **110**, 271–277.

Altintas, Y., Prediction of cutting forces and tool breakage in milling from feed drive current measurements. *ASME Trans. J. Eng. Ind.*, 1992, **114**, 386–392.

Balazinski, M., Czogala, E., Jamielnaik, K. and Leski, J., Tool condition monitoring using artificial intelligence. *Eng. Appl. Artif. Intel.*, 2002, **15**, 73–80.

Bukkapatnam, S.T.S., Kumara, S.R.T. and Lakhtakia, A., Fractal estimation of flank wear in turning. *ASME J. Dyn. Syst. Meas. Cont.*, 2000, **122**, 89–94.

Chen, S.-L. and Jen, Y.W., Data fusion neural network for tool condition monitoring in CNC milling machining. *Int. J. Mach. Tool Manuf.*, 2000, **40**, 381–400.

Dimla Sr, D.E., Sensor signals for tool wear monitoring in metal cutting operations: review of methods. *Int. J. Mach. Tool Manuf.*, 2000, **40**, 1073–1098.

Dimla Sr, D.E. and Lister, P.M., On line metal cutting tool condition monitoring. I: tool state classification using multiplayer perception neural networks. *Int. J. Mach. Tool Manuf.*, 2000a, **40**, 739–768.

Dimla Sr, D.E. and Lister, P.M., On line metal cutting tool condition monitoring. II: force and vibration analysis. *Int. J. Mach. Tool Manuf.*, 2000b, **40**, 769–781.

Dutta, R.K., Paul, S. and Chattopadhyay, A.B., Applicability of the modified back propagation algorithm in tool condition monitoring for faster convergence. *J. Mat. Proc. Tech.*, 2000a, **98**, 299–309.

Dutta, R.K., Paul, S. and Chattopadhyay, A.B., Fuzzy controlled backpropagation neural network for tool condition monitoring in face milling. *Int. J. Prod. Res.*, 2000b, **38**(13), 2989–3010.

Elbestawi, M.A., Marks, J. and Papazafiriou, T., Process monitoring in milling using pattern recognition. *Mech. Syst. Sig. Proc.*, 1989, **3**, 305–315.

Ertunc, H.M., Loparo, A. and Ocak, H., Tool wear condition monitoring in drilling operations using hidden Markov models (HMMs). *Int. J. Mach. Tool Manuf.*, 2001, **41**(9), 1363–1384.

Ghosh, N., Ravi, Y.B., Patra, A., Mukhopadhyay, S., Paul, S., Mohanty, A.R. and Chattopadhyay, A.B., Estimation of tool wear in a CNC milling machine using Neural Network based sensor fusion. *Mech. Syst. Sig. Proc.* (in press).

Inasaki, S.A. and Fuduoka, S., Monitoring system for cutting tool failure using an acoustic emission sensor. *Int. J. of JSME*, 1987, **30**, 523–528.

Jeong, Y.-H. and Cho, D.-W., Estimating cutting force from rotating and stationary feed motor currents on a milling machine. *Int. J. Mach. Tool Manuf.*, 2002, **42**(14), 1559–1566.

Kamarthi, S.V., Kumara, S.R.T. and Cohen, P.H., Flank wear estimation in turning through wavelet representation of acoustic emission signals. *J. Manuf. Sci. Eng.*, 2000, **122**(1), 12–19.

Karuda, S. and Bradley, C., A review of machine vision sensors for tool condition monitoring. *Compu. Indust.*, 1997, **34**, 55–72.

Lathi, B.P., *Communication Systems*, 1968 (John Wiley: London).

Lee, J.M., Choi, D.K. and Chu, C.N., Real time tool breakage monitoring for NC milling processes. *Ann. CIRP*, 1995, **219**, 59–62.

Li, X, Tso, S.K. and Wang, J., Real-time tool condition monitoring using wavelet transforms and fuzzy techniques. *IEEE Trans. SMC Part III*, 2000, **30**(3), 352–357.

Montgomery, D.C., Peck, E.A. and Vining, G.G., *Introduction to Linear Regression Analysis*, 2003 (John Wiley: New York, NY).

Pittner, S., Kamarthi, S.V. and Gao, Q., Wavelet networks for sensor signal classification in flank wear assessment. *J. Intel. Manuf.*, 1998, **9**(4), 315–322.

Prickett, P.W. and Johns, C., An overview of approaches to end-milling tool monitoring. *Int. J. Mach. Tools Manuf.*, 1999, **39**, 105–122.

Romerio-Troncoso, R.J., Herrera-Ruiz, G., Terol-Villalobos, I. and Jaueregui-Correa, J.C., Driver current analysis for sensorless tool breakage monitoring of CNC milling machines. *Int. J. Mach. Tool Manuf.*, 2003, **43**, 1529–1534.

Saglam, H. and Unuvar, A., Tool condition monitoring in face milling based on cutting forces by a neural network. *Int. J. Prod. Res.*, 2003, **41**, 1519–1532.

Scheffer, C. and Heyns, P.S., Wear monitoring in turning using vibration and strain measurements. *Mech. Syst. Sig. Proc.*, 2001, **15**(6), 1185–1202.

Sengupta, D. and Jammalamadaka, S.R., *Linear Models: An Integrated Approach*, 2003 (World Scientific: New York, NY).

Sick, B., On-line and indirect tool wear monitoring in turning with artificial neural networks: a review of more than a decade of research. *Mech. Syst. Sig. Proc.*, 2002, **16**(4), 487–546.

Sun, J., Hong, G.S., Rahman, M. and Wong, Y.S., Identification of feature set for effective tool condition monitoring by acoustic emission sensing. *Int. J. Prod. Res.*, 2004, **42**(5), 901–918.

Szecsi, T., Automatic cutting-tool condition monitoring on CNC lathes. *J. Mat. Proc. Tech.*, 1998, **77**, 64–69.

Ulsoy, A.G. and Koren, Y., Control of machining process. *ASME J. Dyn. Syst. Meas. Cont.*, 1993, **115**, 301–308.

Wang, L., Mehrabi, H.G. and Kannatey-Asibu, E., Hidden Markov model-based tool wear monitoring in turning. *J. Manuf. Sci. Eng.*, 2002, **124**(3), 651–658.